The axisymmetric jet in a rotating reference frame

A Lawrie, Matias Duran-Matute, J Scott, Fabien S. Godeferd, Jan-Bert Flór, C Cambon, Luminita Danaila

▶ **To cite this version:**

A Lawrie, Matias Duran-Matute, J Scott, Fabien S. Godeferd, Jan-Bert Flór, et al.. The axisymmetric jet in a rotating reference frame. Journal of Physics: Conference Series, 2011, 318 (3), pp.032048. ⟨10.1088/1742-6596/318/3/032048⟩. ⟨hal-02140444⟩

HAL Id: hal-02140444

https://hal.science/hal-02140444v1

Submitted on 23 Sep 2020

HAL is a multi-disciplinary open access archive for the deposit and dissemination of scientific research documents, whether they are published or not. The documents may come from teaching and research institutions in France or abroad, or from public or private research centers.

L'archive ouverte pluridisciplinaire **HAL**, est destinée au dépôt et à la diffusion de documents scientifiques de niveau recherche, publiés ou non, émanant des établissements d'enseignement et de recherche français ou étrangers, des laboratoires publics ou privés.

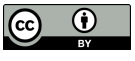

Distributed under a Creative Commons CC BY 4.0 - Attribution - International License

The axisymmetric jet in a rotating reference frame.

A G W Lawrie[1], M Duran-Matute[2], J F Scott[1], F Godeferd[1], J-B Flor[2], C Cambon[1] and L Danaila[3]

[1] LMFA, Ecole Centrale de Lyon
[2] LEGI, Universite Joseph Fourier, Grenoble
[3] CORIA, Universite de Rouen

E-mail: andrew.lawrie@ec-lyon.fr

Abstract. The axisymmetric jet is a geometrically simple, statistically stationary example of inhomogenous turbulence. Considering conservation of volume and momentum, Morton *et al.* (1956) offered a prediction of jet development, characterised solely by an unknown, constant entrainment coefficient. The presence of background rotation complicates the kinematics of the entrainment, and without special treatment, the jet suffers a helical instability. Here, we present one technique which stabilises the axisymmetric jet, yet preserves its desirable turbulent properties. The jet offers a steady-state flow in which there is an axial variation of local Rossby number, and after decay along the axis to a critical value, cones of inertial waves emerge. In this paper, we demonstrate these features using our numerical software MOBILE, offer our solution to stabilise the jet, and explain the mechanisms involved.

1. Introduction

Turbulence in rotating fluids has attracted the attention of many researchers since the experimental work of Hopfinger *et al.* (1982) in which turbulence was created by continuously oscillating a grid by a small amplitude in a large tank. Rossby and Reynolds numbers decayed away from the grid due to viscous dissipation. However, critical questions arising from this work have remained unanswered for three decades, particularly regarding the interaction of turbulence and waves. More recent work by Davidson *et al.* (2006) examined the problem from a different angle, choosing to study the emergence of structures from a region of decaying, rather than continuously forced turbulence. This has the obvious advantage that the turbulence can freely evolve for a few eddy-turnovers before the Rossby number is sufficiently low to generate wave-like structures, thus reducing the influence of spatial and temporal forcing of the grid. Our present work is a novel configuration which imposes neither spatial scales nor temporal forcing, maintains steady-state inhomogenous rotating turbulence, and has a spatially varying Rossby number.

In this paper, we consider an axisymmetric jet with its axis coincident with the axis of rotation of the whole system, and use cylindrical coordinates $(\mathbf{e}_r, \mathbf{e}_\theta, \mathbf{e}_z)$, where z is the coordinate along the axis of the jet. In the case without background rotation, $u_{jet} \sim \frac{1}{z}$ and $r_{jet} \sim z$, as shown by Morton *et al.* (1956), and thus, the nominal jet Reynolds number is constant. Provided the structure of the jet remains unaffected by a background rotation, this would imply in the rotating case that the Rossby number $Ro \sim \frac{1}{z^2}$. This combination of Re and Ro in a statistically stationary, unforced, and self-similar flow makes the jet a remarkably clean testcase for analysis

of turbulence under the influence of the Coriolis force, since structural changes in the turbulence are, unlike grid generated turbulence for example, a function of one variable only. In contrast also to the plethora of work on swirling jets for applications to flame stabilisation, here, the influence of rotation increases (rather than decreases) with axial distance, and thus is robustly maintained long after the jet has 'forgotten' the effects of its emission from a finite aperture.

The following section describes the mechanism of instability we observe in the axisymmetric jet under the influence of rotation and presents an elegant solution to stabilise the jet, which we then compare with results from our MOBILE simulations.

2. Mechanisms

2.1. Azimuthal kinematics

Despite the immediate attractiveness of this testcase, a complication arises due to the jet entrainment. The entrainment flow at sufficiently large distance from the jet axis can be characterised as an axial sink with constant strength, assuming the axial variation of entrainment coefficient is small, and the large-scale flow in an infinite domain is approximately two-dimensional. In the inertially-fixed reference frame, the planetary vorticity gives the initial circulation Γ_0 around each circumferential contour at radius r a finite value,

$$\Gamma_0 = \oint (\mathbf{\Omega} \times \mathbf{r}).\mathbf{ds}, \tag{1}$$

where $\mathbf{ds} = rd\theta\mathbf{e}_\theta$ is a contour element, $\mathbf{\Omega} = [0, 0, \Omega]$ is the rate of solid body rotation, and $\mathbf{r}$ is the position vector of a point on the contour. Kelvin's circulation theorem demands that the circulation on all material contours remains unchanged, ie.

$$\frac{D\Gamma}{Dt} = 0, \tag{2}$$

so as contours converge towards the axial sink, their radius reduces and it follows that the velocity component $\mathbf{u}.\mathbf{ds}$ must increase to preserve the initial circulation. It is clear, therefore, that the far-field effect of the axial sink is amplification of the background vorticity, and that the far-field flow around our jet behaves rather similarly to the far-field flow induced by a tornado. We note that the near-field behaviour is not well-represented by an axial sink, and thus we do not require specific treatment of the singularity at the origin. Neglecting viscosity, the kinematics of the far-field are unbounded in time, since the circulation associated with each contour increases with radius, and contours at all radii eventually converge to the axis.

Naturally we can neither numerically nor experimentally verify our analysis of the far-field in an unbounded domain; however, with our jet in a finite, enclosed domain, we observed azimuthal acceleration of the flow consistent with this idealised analysis. In a finite domain we also observe a helical instability; the jet initially grows, entrains ambient fluid which follows the far-field behaviour discussed above, and this helically displaces the jet from the axis. At large displacement amplitude, the jet breaks down, and the associated entrainment flow ceases. With nothing to drive further radial convergence of material contours, the azimuthal velocity decays sufficiently for the jet to reform, and a periodic formation/breakdown cycle is established.

The key development that lays the basis for our work on steady-state inhomogenous rotating turbulence, is the stabilisation of the far-field flow. Ultimately the problem can be recast as ensuring by some means that the circulation near the axis remains bounded in time. One simple way to achieve this in a finite domain is to enforce radial inflow (ie. no azimuthal velocity) at some distance r_{dom} from the jet, thus limiting the maximum circulation to $\oint |\mathbf{\Omega} \times \mathbf{r}_{dom}| .\mathbf{ds}$, and satisfying continuity by evacuating fluid through a plane at suitably large z. While appropriate

for a finite domain, as one requires in an experiment, there are obvious theoretical and practical limitations to this approach. Instead we focus on a much more elegant solution.

We begin by recognising that in the spatially unbounded problem, contours converge from infinity, and we obtain persistent azimuthal acceleration over time. If one were able to modify the problem such that contours converge from a constant and finite radius, one would recover a steady-state with finite circulation near the axis. We achieve this transformation by adding a small axial velocity u_a to the ambient fluid, rather like a co-axial jet with an outer flow of infinite radius. In the inertially fixed reference frame, flow emanating from the boundary plane has velocity,

$$\mathbf{u}_{ambient} = \Omega r \mathbf{e}_\theta + u_a \mathbf{e}_z, \tag{3}$$

thus material contours emerge from a bottom boundary plane in solid body rotation, and converge towards the axis in space. Contours of small initial radius reach the axis at low values of z and have relatively little circulation, those with larger initial radii reach the axis at larger values of z with greater circulation. The key to this spatio-temporal transformation is that everywhere except for the contour at infinite initial radius, the azimuthal velocity obtained near the axis remains finite and invariant with time, though increasing with z. It is perhaps clearer in the rotating frame to see why the velocities are bounded. If the relative circulation Γ' is defined to be zero in solid body rotation, then by considering the projection onto a plane with the z-axis as its normal, we can use Stokes' theorem to transform the line integral around the contour into a double integral across the enclosed, projected area, A. By projecting the relative velocity field onto the same plane, we obtain an evolution equation for the relative circulation,

$$\frac{D\Gamma'}{Dt} = -\iint 2\Omega \nabla_{2D}.\mathbf{u}' dA, \tag{4}$$

where ∇_{2D} operates solely on the in-plane relative velocity components. Here, one can see that the relative circulation of a material contour is determined by the time-integral of the sink strength within the contour for the duration of travel of the contour from initial to final radius. Thus, if material contours emanate from a boundary at finite radius, their azimuthal velocity remains bounded.

2.2. Kinematics in the (r, z) plane

By considering continuity along individual stream-tubes, the above arguments quite clearly generalises to the case of axially varying sink strength, which corresponds to the situation one might expect from axially developing turbulent anisotropy. The streamline behaviour outside the jet arises from the balance of entrainment and axial co-flow, and since the azimuthal velocity u_θ is perpendicular to the (r, z) plane and independent of θ, we expect the u_r and u_z components of velocity to be approximately irrotational in the interior.

By construction the co-flow imposes a streamfunction boundary condition $\Psi(r, 0) \sim r^2$, and modelling the jet entrainment as a line sink corresponds to $\Psi(r^*, z) \sim z$, where r^* represents the edge of the jet. Since we require axial co-flow, it follows that the streamfunction is not analytic at $(r^*, 0)$, and to resolve this we need to add a point vortex, analogous to a Kutta condition on the boundary. The lateral far-field boundary is somewhat simpler; the streamline at $r = \infty$ takes infinitely long to reach the axis, and thus is vertical with $\Psi = const.$. The schematic in figure 1 illustrates how one might expect the far-field streamline pattern to appear, and shows the contour at infinity as a dashed line.

2.3. Jet dynamics in the high Rossby number region

The volume and axial momentum conservation arguments originally proposed by Morton *et al.* (1956) also appear to hold in the transformed case, since one might assume that the local

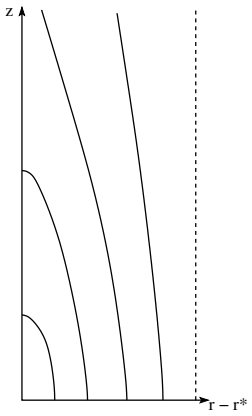

Figure 1. Far-field streamline pattern, modelling the jet as an axial sink.

entrainment is not affected by the shape of the entrained stream-tube in the far-field. This is a reasonable assumption provided the characteristic eddy velocity is significantly faster than the azimuthal velocity of the entrained fluid at the edge of the jet. By conserving circulation it is trivial to show that the azimuthal velocity of a material contour originating at radius r is given by

$$u_\theta = \frac{\Omega r^2}{r^*}, \tag{5}$$

where r^* is its current radius. If r^* is taken as the edge of the jet, $r^* \sim z$, and noting that all volume emanating from the bottom boundary eventually reaches the axis, $r \sim z^2$, then

$$u_\theta \sim z^3. \tag{6}$$

There exists therefore a region in which our original assumption is valid, sufficiently far from the origin (we require that the jet commences with a finite aperture to circumvent the singularity at the axis), but before $u_{jet} - u_a \sim O(u_\theta)$.

2.4. Jet dynamics in the low Rossby number region

Once the Rossby number of the jet approaches order unity, both the core jet flow and the relatively slow entrained flow are influenced by rotation. It is well-known that inertial waves propagate from eddies in a rotating ambient, though the mechanism of generation has been the focus of widespread debate in recent years. In the rotating reference frame, one obtains the form of a linear wave equation by neglecting the nonlinear $\mathbf{u}.\nabla\mathbf{u}$ term in the momentum equation, ie.

$$\frac{\partial^2 \hat{\mathbf{u}}}{\partial t^2} + \bar{\omega}^2 \hat{\mathbf{u}} = 0, \tag{7}$$

where $\hat{\mathbf{u}}$ is the relative velocity field Fourier-transformed onto a set of basis vectors $\mathbf{k}$, and $\bar{\omega}$ has dimensions of $\frac{1}{T}$. The dispersion relation,

$$\bar{\omega} = \pm \frac{2\mathbf{\Omega}.\mathbf{k}}{|\mathbf{k}|}, \tag{8}$$

is unusual, since surfaces of constant phase ripple in the direction of the phase velocity,

$$\mathbf{c}_p = \frac{\bar{\omega}\mathbf{k}}{\mathbf{k}.\mathbf{k}} = \pm \frac{2(\mathbf{\Omega}.\mathbf{k})\mathbf{k}}{|\mathbf{k}|^3}, \tag{9}$$

while energy is transported in the direction of the group velocity,

$$\mathbf{c}_g = \nabla\bar{\omega}(k) = \pm\frac{2\mathbf{k}\times(\mathbf{\Omega}\times\mathbf{k})}{|\mathbf{k}|^3}, \tag{10}$$

and it can be shown that the two directions are perpendicular. As demonstrated very beautifully in Godeferd & Lollini (1999), inertial waves propagate in axisymmetric cones of constant angle to the rotation axis, with equatorial wave-vectors $\mathbf{k}$ corresponding to axial propagation, and axial wave-vectors being the limiting case of slow, radially propagating inertial waves. The axisymmetry of our jet configuration is thus a very powerful feature, since it corresponds directly to the physical nature of the inertial waves. In homogenous turbulence, one can conceive of a sea of inertial waves of all directions, with, on average, all incoming and outgoing inertial waves destructively interfering. This elegant symmetry is unavailable in inhomogenous cases such as our jet. Waves that propagate with group velocities at angles close to the rotation axis remain within the jet and interact with the turbulence, but those that radiate more horizontally leave the jet, remove energy, and act as an angular filter on wave-turbulence interactions.

3. Results

3.1. Computational method

Following the Large Eddy Simulation work of Lawrie & Dalziel (2011*a*,*b*), for our preliminary calculations presented here, we use a third order, staggered grid, fractional step methodology to solve the following equations of motion in the relative frame,

$$\frac{\partial(\rho u_i')}{\partial t} + \frac{\partial \rho u_i' u_j'}{\partial x_j} = -\frac{\partial p'}{\partial x_i} + 2\epsilon_{ijk}u_j'\Omega_k \tag{11}$$

subject to the constraint

$$\frac{\partial u_i'}{\partial x_i} = 0, \tag{12}$$

which is enforced exactly through a pressure re-distribution at each timestep. A parallel multigrid scheme is used to accelerate the pressure convergence. We use stress-free zero flux conditions on the side-walls of the domain to mimic the pressure field of our computational setup while neglecting the influence of thin boundary layers on the walls, and an inflow boundary condition that represents both the unswirled ambient inflow and the nozzle aperture. The outflow is a balanced flux, stress-free condition approximately transmissive to inertial waves with a spatial frequency well-resolved on the mesh. In the calculation we present here, the mesh was formed from cubic cells, $256 \times 256 \times 1024$, with the large direction aligned with the nozzle and the rotation axis. Even with this size of calculation, the nozzle aperture occupies only $O(10)$ cells of the boundary surface, and hence this region is inadequately resolved. However, in the critical Rossby number regions that are of specific interest in this work, the inertial waves, the integral scale of the turbulence and perhaps a decade of inertial range are well resolved.

3.2. Discussion

The numerical work we present here is part of a larger collaborative effort to study the evolution of anisotropic turbulence, and the stabilised jet configuration is the focus of the numerical and experimental components thereof. We show with our preliminary calculations firstly that a quasi-steady state can indeed be achieved for the co-flowing jet, and secondly that our key scalings are well-matched by the data.

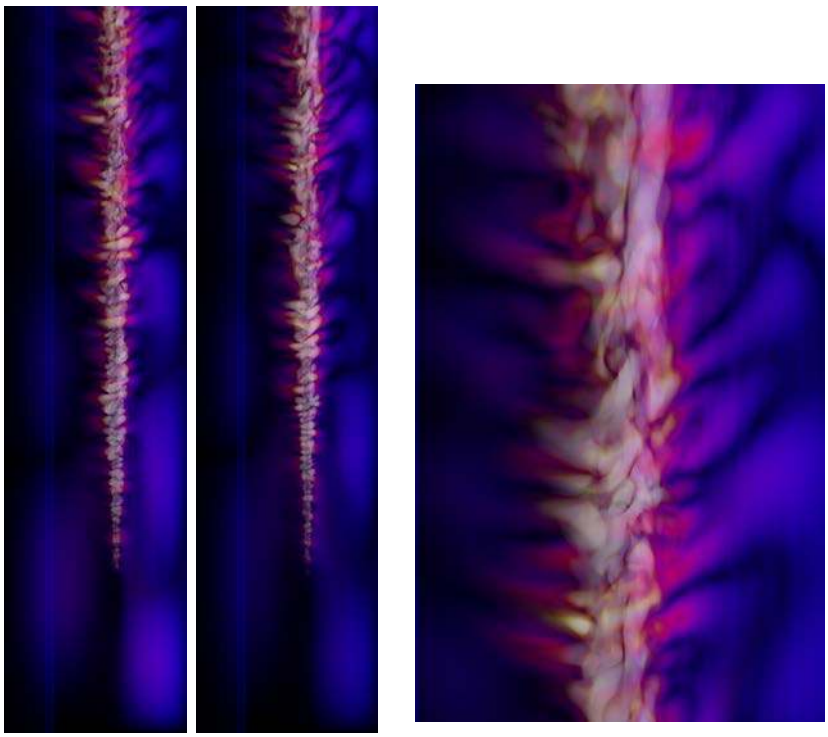

Figure 2. False-colour perspective rendering of radial velocity in a thin volume at $\frac{t}{2\pi\Omega} =$ (left) 3, (middle) 6, and (right) a close-up of (middle) in the low Rossby number region, detailing eddy elongation by inertial waves towards the edge of the jet.

In figure 2, which renders radial velocity in a thin volume around the jet axis, by comparing the plots taken at times $\tau_\Omega = 3$ and $\tau_\Omega = 6$, where $\tau_\Omega = \frac{t}{2\pi\Omega}$. The other parametric time-scale in the problem is the axial advection time-scale $\tau_z = \frac{z_{dom}}{u_a}$, and for the simulation shown the corresponding values are $\tau_z = 1.25$ and $\tau_z = 2.5$. The testcase selected here uses $\frac{u_j}{u_a} = 4$ and for this relatively large co-flow velocity ratio, the velocity field does not display the strong helical instability of the zero co-flow case, despite there being a strong and vertically increasing azimuthal velocity. The spread angle of the jet, with respect to the classical Morton *et al.* (1956) model, is reduced by the co-flow. In common with non-rotating co-flowing jets, the temporal rate of increase in jet radius is maintained by entrainment, but the axial advection reduces the spatial rate of growth, leading to its distinctive, shallow angle form. We performed this calculation in a large-aspect-ratio domain, to ensure that we captured the important jet development regimes, and that we can quantify deviation from our scalings due to the confinement of the computational domain.

In an unconfined domain, material contours approaching the axis at continuously increasing z emanate from continuously increasing r, but this is no longer possible when there is a radial limit to the domain, and thus r_{dom} sets the maximum circulation of any entrained contour, and hence bounds u_θ. In cases where the volume flux that it is possible for an unconfined jet to entrain is a significant proportion of the co-flow volume flux, we expect a laterally confined case to exhibit reduced entrainent. In the calculation presented in figure 2 we chose u_a such that the volume flux entrained into the jet is weak relative to the co-flow volume flux, so accordingly we expect negligible adjustment of the entrainment. Figure 3 shows the actual azimuthal velocity, and there are several points of interest to be noted here. The resolution of the flow in the

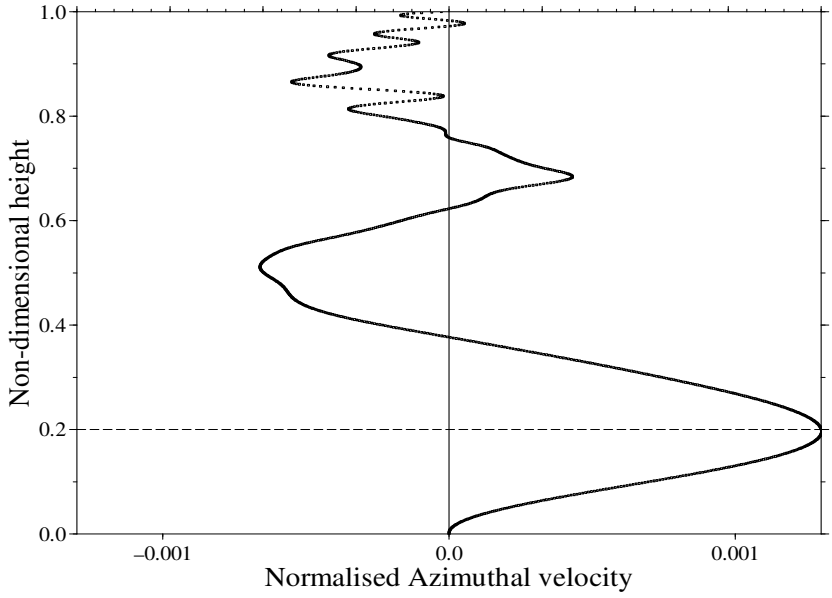

Figure 3. Azimuthal velocity averaged over planar annuli $0.35r_{dom} > r > 0.3r_{dom} > r_{jet}$ as a function of height, normalised by $\Omega r_{dom}^2/\overline{r}$. The location of the virtual origin is shown by a dashed line.

vicinity of the nozzle is too poorly resolved to allow turbulence to develop immediately in a natural manner, and consequently the entrainment flow cannot develop either. The virtual origin that arises is located at $z = 0.2$, and one can consider this as being analogous to the location of a nozzle aperture. Interestingly, in this situation where axial co-flow is only enforced some distance behind the 'nozzle', one obtains a vertically inhomogeneous axial sink. Thus streamlines in (r, z) emanating from the bottom boundary must converge towards the bottom extremity of the sink, and this induces anti-cyclonic azimuthal velocity (vortex compression). Once the entrainment flow begins, at $z > 0.2$, $\frac{\partial u_\theta}{\partial z}$ becomes positive and follows the z^3 prediction closely (vortex stretching). At sufficiently large z, it becomes aware of the finite lateral boundary, and u_θ ceases to increase monotonically.

The most valuable feature that we encounter is the Rossby number variation with axial distance. While this does occur in swirling jets (used for instance to stabilise flames), there, the influence of rotation decays rapidly as the initial circulation is diffused radially by turbulent transport, and so low Rossby numbers are restricted to a region close to the nozzle, and it becomes difficult to separate effects caused by a finite aperture nozzle from those caused by rotation. In our novel case, however, the jet approaches a self-similar form some distance downstream of the nozzle, but with appropriate selection of rotation rates, this occurs well before the Rossby number falls below a critical value. As noted earlier, substantial under-resolution of turbulent scales close to the nozzle leads to a large displacement of the virtual origin, and here, such separation of length-scales is particularly desirable. Figure 4 shows the Rossby number as a function of height, measured from the turbulent integral length- and velocity-scales,

$$Ro_{turb} = \frac{u_{turb}}{\Omega l_{turb}}, \tag{13}$$

and it follows reassuringly closely the scaling we predicted in the introduction by extrapolating from the non-rotating non-co-flowing jet. Thus we can examine the transition from turbulent

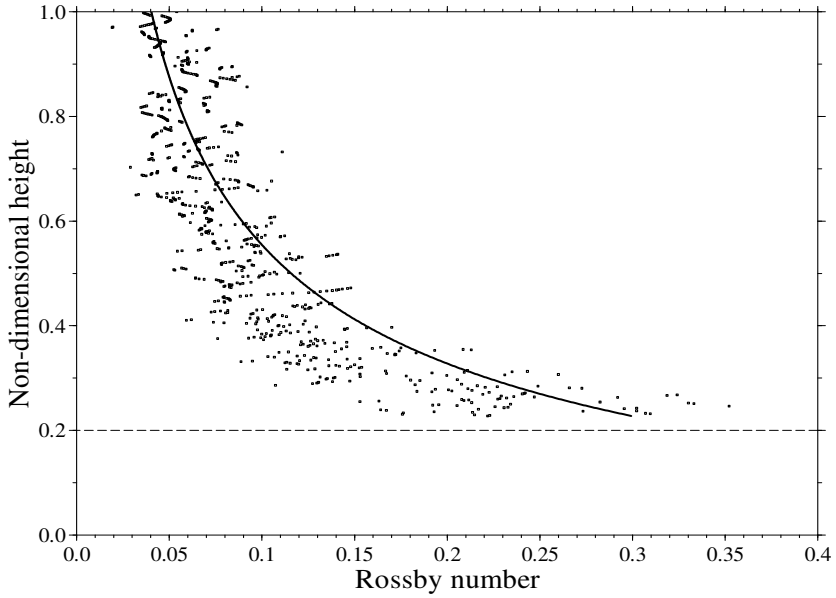

Figure 4. Rossby number as a function of height, with $Ro \sim \frac{1}{z^2}$ scaling superimposed.

isotropy to anisotropy simply by reading off time-averaged statistics at each axial position.

4. Conclusions

In this paper we have presented, for the first time to our knowledge, a means of obtaining unforced statistically stationary rotating turbulence together with a means of varying Rossby number in space rather than in time in a spatially self-similar flow. Our approach uses a free jet subject to background rotation and while the most obvious configuration leads to unbounded azimuthal acceleration, a small modification mitigates this effect and thus the concept has practical utility. As part of a larger collaborative study on anisotropic turbulence, combining theoretical, numerical and experimental tools, we present our initial findings from our numerical software MOBILE on our novel jet configuration.

5. Acknowledgments

The authors would like to thank the French National Research Agency, ANR for their financial support through the project ANISO for this collaboration.

References

Davidson, P. A., Staplehurst, P. J. & Dalziel, S. B. 2006 On the evolution of eddies in a rapidly rotating system. *J. Fluid Mech.* **557**, 135–144.

Godeferd, F. S. & Lollini, L. 1999 Direct numerical simulations of turbulence with confinement and rotation. *J. Fluid Mech.* **393**, 257–308.

Hopfinger, E. J., Browand, F. K. & Gagne, Y. 1982 Turbulence and waves in a rotating tank. *J. Fluid Mech.* **125**, 505–534.

Lawrie, A. G. W. & Dalziel, S. B. 2011*a* Turbulent diffusion in tall tubes, Part I: models for Rayleigh-Taylor instability. *Phys. Fluids (accepted)* .

Lawrie, A. G. W. & Dalziel, S. B. 2011*b* Turbulent diffusion in tall tubes, Part II: confinement by stratification. *Phys. Fluids (accepted)* .

Morton, B., Taylor, G. I. & Turner, J. S. 1956 Turbulent gravitational convection from maintained and instantaneous sources. *Proc. R. Soc.* **234**, 1–23.